Development of a Two-Dimensional Zonally Averaged Statistical–Dynamical Model. Part II: The Role of Eddy Momentum Fluxes in the General Circulation and their Parameterization

PETER H. STONE

Center for Meteorology and Physical Oceanography, Massachusetts Institute of Technology, Cambridge, MA 02139 and NASA/Goddard Space Flight Center, Institute for Space Studies, New York, NY 10025

MAO-SUNG YAO

Centel Business Information Systems, Inc., NASA/Goddard Space Flight Center, Institute for Space Studies, New York, NY 10025

(Manuscript received 29 April 1987, in final form 21 July 1987)

ABSTRACT

The effect of eddy momentum fluxes on the general circulation is investigated with the aid of perpetual January simulations with a two-dimensional, zonally averaged model. Sensitivity experiments with this model show that the vertical eddy flux has a negligible effect on the general circulation, while the meridional eddy flux has a substantial effect. The experiments on the effect of the meridional eddy flux essentially confirm the results found by Schneider in a similar (but not identical) set of sensitivity experiments, and, in addition, show that the vertical structure of the meridional eddy flux has a relatively small effect on the general circulation.

In order to parameterize the vertically integrated meridional eddy momentum flux, we take Green's parameterization of this quantity and generalize it to allow for the effects of condensation. In order to do this, it is necessary to use Leovy's approximation for the eddy fluctuations in specific humidity. With this approximation the equivalent potential vorticity defined by Saltzman is conserved even when condensation occurs. Leovy's approximation also allows one to generalize the relation between quasi-geostrophic potential vorticity and the Eliassen–Palm flux by replacing the potential vorticity and potential temperature by the corresponding equivalent quantities. Thus, the eddy momentum flux can be related to the eddy fluxes of two conserved quantities even when condensation is present. The eddy fluxes of the two conserved quantities are parameterized by mixing-length expressions, with the mixing coefficient taken to be the sum of Branscome's mixing coefficient, plus a correction which allows for nonlinear effects on the eddy structure and ensures global momentum conservation.

The parameterization of the meridional eddy transport is tested in another perpetual January simulation with the two-dimensional averaged model. The results are compared with a parallel three-dimensional simulation which calculates the eddy transport explicitly. The parameterization reproduces the latitudinal and seasonal (interhemispheric) variations and the magnitude of the eddy transport calculated in the three-dimensional simulation reasonably well.

1. Introduction

This is the second paper in a series describing a two-dimensional (2-D), zonally averaged, statistical-dynamical climate model being developed at the Goddard Institute for Space Studies (GISS). This model's structure and parameterizations have much in common with the GISS three-dimensional (3-D) climate model (Hansen et al., 1983). However, the 2-D model is almost two orders-of-magnitude faster than the 3-D model, and therefore can be applied to problems for which the 3-D model is not well suited; e.g., problems requiring many parameter variations, very long time integrations, or coupling with complex chemical models.

The basic description of the model and the philosophy behind it are given in the first paper in this series (Yao and Stone, 1987, hereafter referred to as Part I). A comprehensive review of other 2-D statistical-dynamical models and the history of their development is given by Saltzman (1978). Our model is distinguished from others of the same kind by its inclusion of a comprehensive hydrological cycle and radiation treatment, high vertical resolution (normally nine levels), and by its parameterizations of moist convection and large-scale eddies.

In Part I we focused on the development of the moist convection parameterization for our 2-D model. In the current paper we concentrate on the development of a parameterization for the zonal mean large-scale meridional eddy flux of momentum. A summary of earlier work on this problem is, again, found in Saltzman (1978). We found that the earlier parameterizations were inadequate, and one major objective of the present paper is to present and test a new parameterization of the eddy momentum flux. Our parameterization is a

generalization of Green's (1970) parameterization, and it also uses Branscome's (1983) results for baroclinic eddy mixing coefficients. In the course of developing our parameterization, we performed a number of sensitivity studies that yielded useful information about the role of eddy momentum fluxes in the general circulation. Thus another major objective of the present paper is to present the results of these sensitivity studies.

The paper is arranged as follows. In section 2 we describe the model, the controls used to evaluate our experiments, and how the experiments were carried out. In section 3 we describe various sensitivity studies involving prescribed changes in the zonal mean eddy momentum fluxes. In section 4 we present our parameterization of the zonal mean meridional eddy flux of momentum, and test it. Finally, in section 5 we summarize our results and conclusions.

2. Design of the experiments

We give here only a brief outline of our 2-D zonally averaged model. A more complete description can be found in Part I. The model solves the primitive equations (including the moisture conservation equation) in sigma and spherical coordinates as an initial value problem. There are nine vertical levels: two in the planetary boundary layer, five in the troposphere, and two in the stratosphere. The model top is at 10 mb, and at higher levels, temperatures are determined by radiative equilibrium. There are 24 grid points in latitude, corresponding to a resolution of 7.826°, and the time step is 15 min. The space and time differencing schemes closely parallel those in the GISS 3-D Model II (Hansen et al., 1983), except that an eighth-order Shapiro filter is used to suppress the two-grid-size noise typical of 2-D models. It is applied to surface pressure and potential temperature once every hour.

Topography is omitted and surface grid points are divided into land, land-ice, ocean, and sea-ice fractions. In general, the sea-ice fraction and the temperatures of the various surface types are calculated interactively. Surface momentum transfer and latent and sensible heat fluxes are calculated separately for the different surface types using conventional drag laws.

Incident solar radiation is specified as a function of time of day, season, and latitude. The radiative calculations include all significant atmospheric constituents, and employ realistic short- and longwave properties. In general, the distributions of water vapor and clouds are calculated, while the remaining radiatively active constituents are specified.

Large-scale condensation and associated clouds and precipitation occur in an atmospheric layer whenever the relative humidity exceeds 100%. Moist convection occurs whenever the moist static energy at one level exceeds the saturated moist static energy at the next higher level. Its effects are parameterized with a penetrative convection scheme which transports sensible heat, moisture, and horizontal momentum between the unstable layers. Any resulting supersaturation leads to condensation and precipitation. The amount of mixing due to moist convection depends on the fraction of a latitude belt which is unstable, and this is calculated from the zonal variance of the moist static energy. This variance is assumed to be due to eddies arising from baroclinic instability, and it is calculated from parameterizations based on baroclinic stability theory.

The eddy momentum and heat fluxes are also in general parameterized, based on the assumption that the eddies arise from baroclinic instability. The parameterization of the eddy momentum fluxes will be described in this paper, and the parameterizations of the eddy heat fluxes will be described in a subsequent paper.

In order to investigate the eddy momentum fluxes and their parameterization, it is not necessary to use the full generality of our 2-D model as just outlined. Therefore, we made the following simplifications for all the experiments reported in this paper. The fractional land areas were set equal to zero at all latitudes; the diurnal cycle was omitted; and the sea-ice fractions, sea-surface temperatures, cloud amounts, eddy wind variances, and eddy fluxes of sensible heat and moisture were specified, i.e., held fixed throughout the integrations. The sea-ice fractions and sea surface temperatures were taken from zonally averaged January mean climatological data. The cloud and eddy statistics were taken from a perpetual January simulation with a semispectral version of the 3-D GISS Model II GCM. This 3-D model differed from the published Model II (Hansen et al., 1983) in two respects. First, the zonal variations were calculated by means of a spectral expansion which retained the first nine zonal wavenumbers, rather than by finite differencing. Second, all zonal variations were removed from the boundary conditions, i.e., the lower boundary was all ocean, having sea-ice fractions and sea surface temperatures independent of longitude. The 3-D perpetual January simulation used the same values for these boundary conditions as the 2-D experiments. This 3-D control run is described in more detail in Part I.

Since the 3-D simulation contained no nonzonal forcing, the eddy fields it produced are appropriate controls for validating parameterizations of eddy statistics which are meant to represent eddies arising from baroclinic instability, rather than from topography and land–ocean contrasts. In particular, we will use the eddy momentum fluxes produced by this 3-D simulation as the standard for evaluating our parameterizations of these fluxes. Figures 1 and 2 illustrate the vertical and meridional eddy momentum fluxes, respectively, produced by this 3-D simulation. They are qualitatively similar to calculations of these fluxes based on observations, e.g., compare with the result of Starr et al. (1970) for the vertical flux and Oort and Rasmusson's (1971) result for the meridional flux. However, they

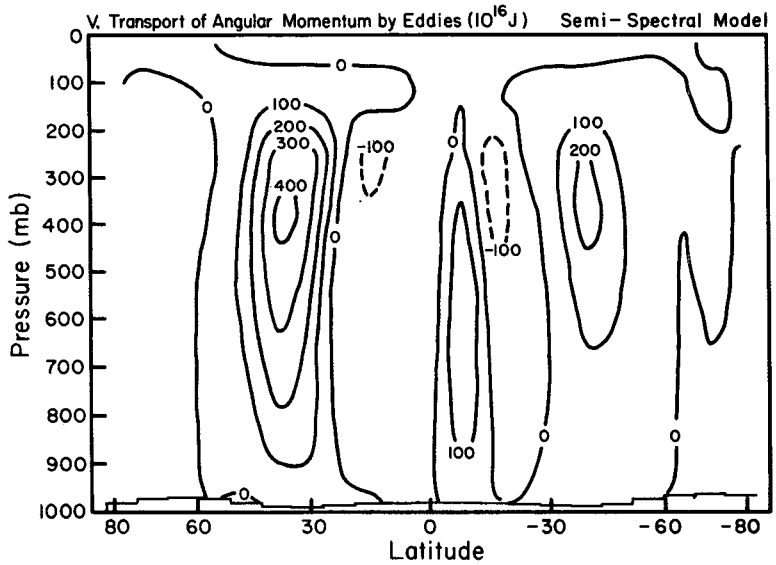

FIG. 1. Pressure-latitude cross section of the zonal mean vertical transport of angular momentum by eddies from the 3-D control run with zonally uniform boundary conditions. Units = 10^{16} J.

cannot be compared in detail with the observations because the latter are affected by feedbacks with stationary eddies, which have been excluded from the 3-D simulation.

Nevertheless, the 3-D model's simulation of the transient eddies can be qualitatively verified by comparing its performance with observations when realistic lower boundary conditions are used in the model simulation. The 3-D semispectral model has, in fact, also been used to simulate a calendar January, with realistic lower boundary conditions for continents, topography and sea-surface temperatures—the same boundary conditions as were used in the Model II simulations reported by Hansen et al. (1983). Some details of this simulation were given in Part I. Figure 3 shows the vertically integrated northward transports of momentum by transient eddies and by all eddies in the Northern Hemisphere, taken both from this simulation, and from January observations (Oort and Rasmussen, 1971). The model's simulation of the transient eddy

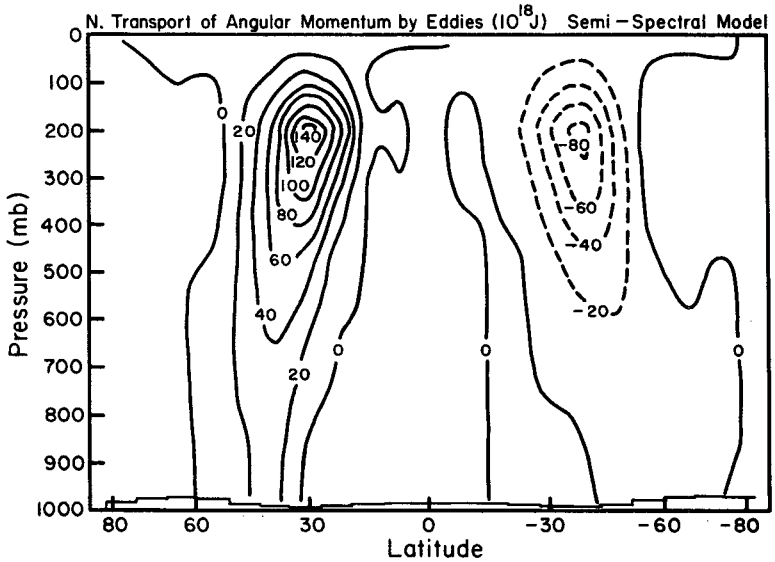

FIG. 2. As in Fig. 1, but for northward transport of angular momentum by eddies. Units = 10^{18} J.

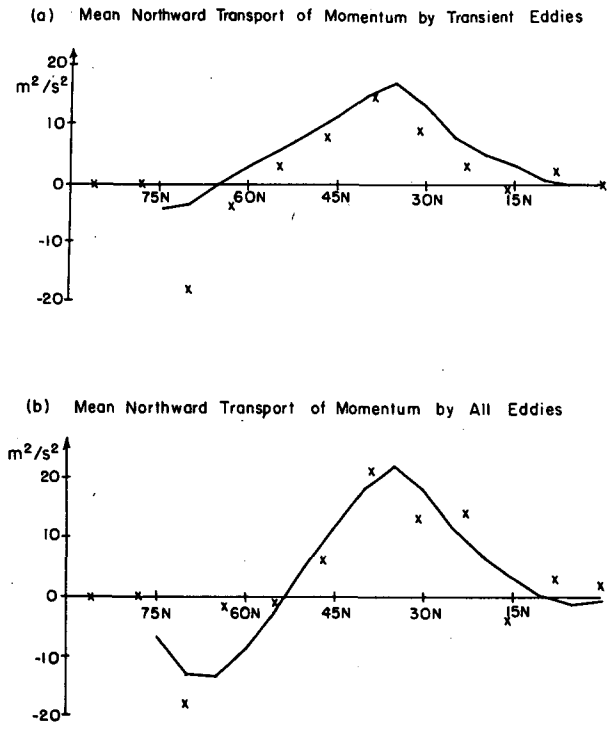

FIG. 3. January mean northward transport of momentum by (a) transient eddies and (b) all eddies vs latitude. Results from observations (Oort and Rasmusson, 1971) are shown by the solid curves, and from the 3-D simulation with realistic boundary conditions by X's.

momentum flux appears reasonable. The one highly anomalous point, near 70°N, illustrates the difficulty in evaluating the model's simulation of transient eddies when stationary ones are present. In fact, the anomaly largely disappears when one compares the total eddy transport with the observations. It is not clear whether it is the model's simulation of the transient or stationary eddies which is primarily at fault, but we suspect it is the latter, since the transient eddy flux at 70°N is well behaved when stationary eddies are omitted (e.g., see Fig. 8). In any case the semispectral model appears to do well in simulating the magnitude and location of the maximum transient eddy momentum transport in midlatitudes.

All the 2-D experiments we describe in this paper were perpetual January simulations paralleling the 3-D simulation with zonal variations in the forcing omitted. In all the perpetual January experiments, either 2-D or 3-D, the initial conditions were actual data for 1 December 1976, and the integrations were carried out for eight months, sufficient for an equilibrium climatology to be established. All the mean fields shown from these experiments are means for the eighth month of these integrations, and all the differences we discuss are much larger than the monthly variations, unless otherwise mentioned.

In all the 2-D experiments the eddy momentum fluxes were changed in various ways, to be described in sections 3 and 4. In interpreting these experiments, one must keep in mind how the experiments have been constructed. In particular, the eddy momentum fluxes do not interact with the eddy fluxes of sensible heat and moisture. Thus, errors in any possible parameterizations of these last two fluxes do not contribute to differences in the experiments. (The parameterizations of these fluxes will be discussed in a subsequent paper.) Also, the radiative heating is essentially fixed, since clouds, sea surface temperatures, and incident solar radiation are all fixed. However, the model includes both hemispheres, and January boundary conditions are used, so the simulations do include both summer and winter conditions. In the experiments the eddy momentum fluxes do interact with moist convection, surface fluxes, large-scale condensation, and the internal longwave radiative fluxes. We showed in Part I that the 2-D model's parameterizations of these processes led to 2-D simulations of the general circulation, surface fluxes, precipitation, and so on, which were in good agreement with those simulated in the 3-D control run.

As a standard for evaluating our subsequent experiments, we illustrate in Fig. 4 the zonal wind field produced by the 2-D model when the eddy momentum fluxes are fixed at the values produced by the 3-D simulation (shown in Figs. 1 and 2). This 2-D control run is identical to the 2-D experiment with the final moist convection parameterization described in Part I. All the 2-D model experiments reported in this paper differ from this control run solely in how the eddy momentum fluxes are specified or calculated.

3. Sensitivity experiments

For convenient reference, Table 1 lists the various model simulations that we focus on in this paper. In the first experiment with the 2-D model, experiment A, the vertical eddy flux of angular momentum was set equal to zero, while the meridional eddy flux was fixed at the values calculated in the 3-D control run. Figure 5 shows the zonal mean zonal wind from this experiment. Comparing it with the zonal wind from the 2-D control run, Fig. 4, one can see very little difference. The only noticeable difference is some increase in the westerlies near the equatorial tropopause and in the easterlies in the equatorial troposphere. Overall, however, the vertical eddy flux of momentum seems to play very little role in the general circulation. This conclusion is confirmed by an examination of the other fields produced in experiment A (not shown).

Starr et al. (1970) estimated the vertical eddy flux of momentum in the atmosphere by calculating what vertical eddy flux was necessary for equilibrium. They noted that this vertical flux made a contribution to the overall momentum balance which was comparable in

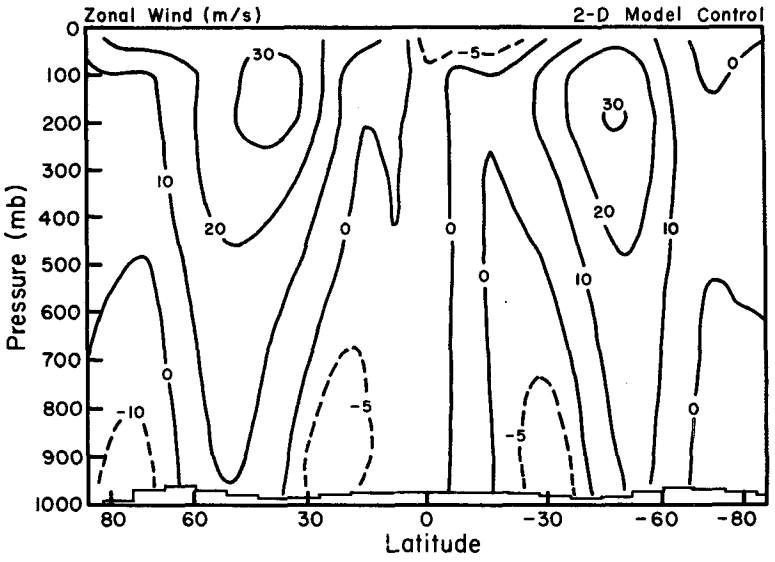

FIG. 4. Pressure–latitude cross section of the zonal mean zonal wind from the 2-D control run. Units = m s^{-1}.

magnitude to the contribution by the meridional eddy flux of momentum, and concluded that the vertical eddy flux had an important impact on the general circulation. This conclusion is not supported by our experiment A, even though the vertical eddy flux calculated by our 3-D control run is similar in magnitude to that calculated by Starr et al. (1973). The reason is that, although the contributions of the vertical and meridional eddy momentum fluxes to the momentum balance in our 3-D control run can be said to be similar in magnitude, in fact the former contribution is only about one-quarter of the latter. We conclude that it is not necessary to parameterize the vertical eddy flux of momentum in order to have a good simulation of the general circulation.

TABLE 1. Model simulations and their treatment of the eddy fluxes of zonal momentum.

Model simulation	Meridional flux	Vertical flux
3-D control run	Calculated explicitly	Calculated explicitly
2-D control run	Taken from 3-D control run	Taken from 3-D control run
2-D experiment A	Taken from 3-D control run	Zero
2-D experiment B	Zero	Taken from 3-D control run
2-D experiment C	Meridional structure taken from 3-D control run; vertical structure independent of height	Taken from 3-D control run
2-D experiment D	Calculated from parameterization for a dry atmosphere	Taken from 3-D control run
2-D experiment E	Calculated from parameterization for a moist atmosphere	Taken from 3-D control run

In a second experiment with the 2-D model, experiment B, the meridional eddy flux of angular momentum was set equal to zero. The zonal mean zonal wind from this experiment is shown in Fig. 6. The zonal winds are now quite different from those in the 2-D control run (see Fig. 4). The midlatitude jets have moved two grid points equatorward (~16°); the Northern Hemisphere jet is 7 m s^{-1} stronger; secondary jets have appeared near the poles in both hemispheres; and two jets have appeared at the equator, an easterly jet near the tropopause, and a weak westerly jet in the middle troposphere.

The major change, the equatorward shift of the midlatitude jets, is just what one would expect to happen, based on current understanding of the role of meridional eddy transports of momentum in the general circulation. The other changes would have been harder to anticipate; they can mostly be understood in the context of the model's momentum balance. The secondary jets near the poles are caused by the removal of the relatively weak equatorward eddy fluxes of momentum near the poles. This change also weakened the direct polar cell and decreased the polar subsidence, leading to temperatures much colder than those in the control run. For example, at 82°N the mean temperature in experiment B was 10° colder.

The weak westerly equatorial jet is forced by the vertical eddy flux of momentum, once the opposing effect of the meridional eddy flux is removed. The easterly jet near the tropopause is caused by very strong meridional winds which developed near the tropopause

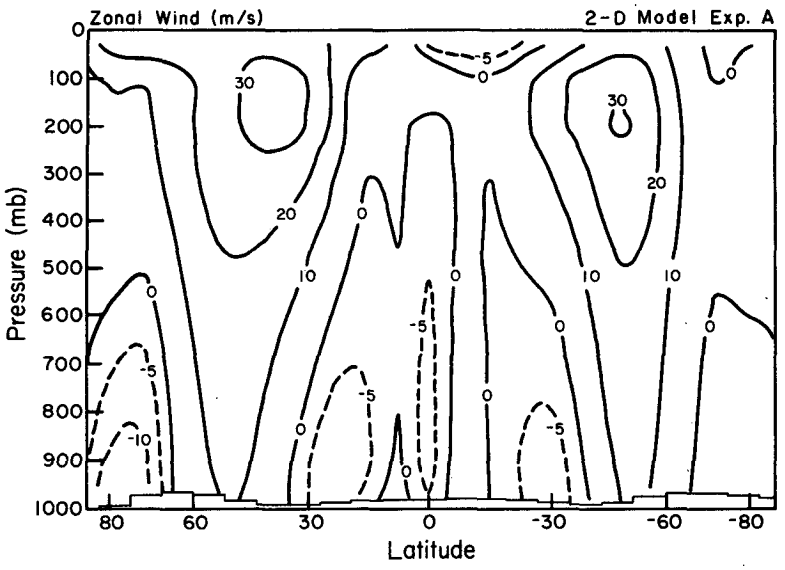

FIG. 5. As in Fig. 4, but with the vertical transport of angular momentum by eddies set equal to zero (experiment A).

and supply the necessary easterly momentum. The strong meridional winds are forced by the asymmetric radiative forcing at the equator in January, and may be unrealistically large because of the constraints we have imposed in the experiment, e.g., the other eddy fluxes are not allowed to adjust to the removal of the meridional eddy flux of momentum. In the control run the asymmetric radiative forcing is sufficiently balanced that strong meridional winds do not occur.

Schneider (1984) has also used a 2-D model to examine what happens when the meridional eddy flux of momentum is omitted from the forcing for the general circulation. Since his experiments used annual mean forcing while ours used January forcing, we cannot directly compare our results with his. In particular, the Hadley circulations play a much larger role in the momentum balance in our experiments than in Schneider's. Nevertheless, in both sets of experiments there is a qualitative agreement, i.e., the midlatitude jets tend to move equatorward and to become stronger. However in Schneider's experiments, the equatorward shift is smaller, and the increase in the maximum zonal

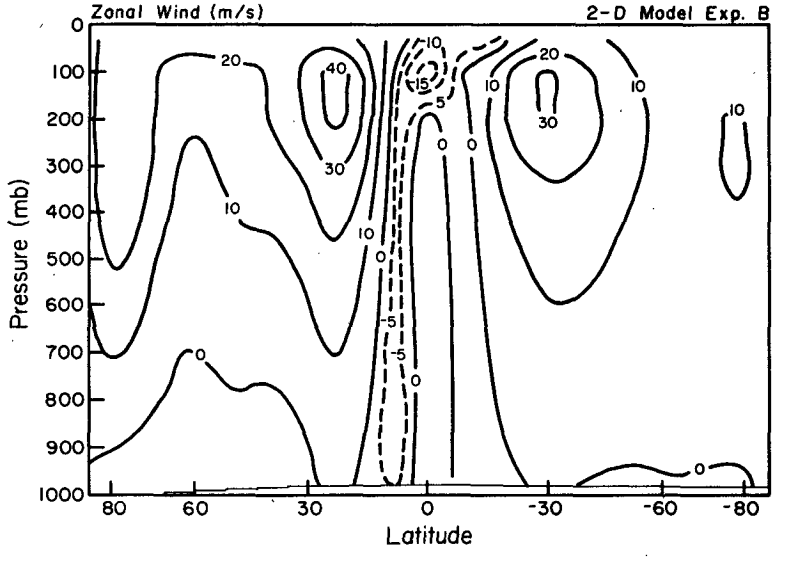

FIG. 6. As in Fig. 4, but with the meridional transport of angular momentum by eddies set equal to zero (experiment B).

winds is greater. Schneider's experiments also showed polar jets developing, but they were much weaker and at lower latitudes than in our experiment. No equatorial jets developed in his experiments, which is consistent with our results, since his forcing was symmetric about the equator, and he omitted any forcing by vertical eddy momentum fluxes.

In addition, Schneider examined the effect of removing the meridional eddy momentum flux on the mean meridional circulations. He found that the Ferrel cells disappeared while the mass circulation in the Hadley cells was virtually unchanged. Our experiment B showed the same changes, except that in the Southern (summer) Hemisphere the strength of the Ferrel cell was reduced by only 60%. This difference is not surprising, since the eddy momentum flux contribution to the forcing of the Ferrel cell is much less in summer than in winter or in the annual mean (Salustri and Stone, 1983).

Schneider also noted that the meridional eddy momentum fluxes tended to minimize the kinetic energy in the zonal mean flow, K_M. Our experiments showed a similar result; i.e., in experiment B, K_M was 28% greater than in the control run in the Northern Hemisphere. (It was also greater in the Southern Hemisphere, but only by 3% which is not statistically significant.) This confirmation of Schneider's result is particularly interesting in view of the fact that the diabatic heating, particularly its dominant component, the convective heating, responds to changes in the eddy momentum flux in our experiments, whereas the diabatic heating was held fixed in Schneider's. In both experiments the eddy heat fluxes were kept fixed.

A third 2-D experiment, experiment C, was designed to see how important the vertical structure of the meridional eddy momentum flux is in determining the flux's effect on the general circulation. In this experiment the mass-weighted vertical integral of the meridional eddy flux was kept the same as in the control run, but the eddy flux per unit mass was made independent of height. We expected that the zonal mean zonal wind in mid- and high latitudes would not be very sensitive to the vertical structure of this flux because the zonal wind's vertical shear is constrained by the thermal wind relation and the surface winds are constrained by surface drag.

Figure 7 shows the mean zonal wind field from experiment C. Comparing this field with that from the control run, Fig. 4, we see that in fact the one major change is in the tropics, where an easterly jet has developed near the tropopause. This jet closely resembles the one that developed in the same location in experiment B, and has the same cause, i.e., the asymmetric radiative forcing at the equator near 100 mb is no longer balanced. By contrast, in mid- and high latitudes, the changes in the mean zonal wind are relatively minor, as expected. In particular, the changes are much smaller than in experiment B (cf. Fig. 6). For example, there is no perceptible shift in latitude of the midlatitude jet streams, and there is only a hint of experiment B's polar jet streams. In experiment C the midlatitude jet streams are only 4 m s^{-1} weaker than in the control run. Similarly the impact on the mean meridional circulations is relatively small. For example, in experiment B the Northern Hemisphere Ferrel Cell disappeared, while in experiment C its strength was unchanged. We conclude that a successful parameterization of the meridional eddy flux of momentum is not strongly dependent on a good parameterization of the vertical structure of the flux.

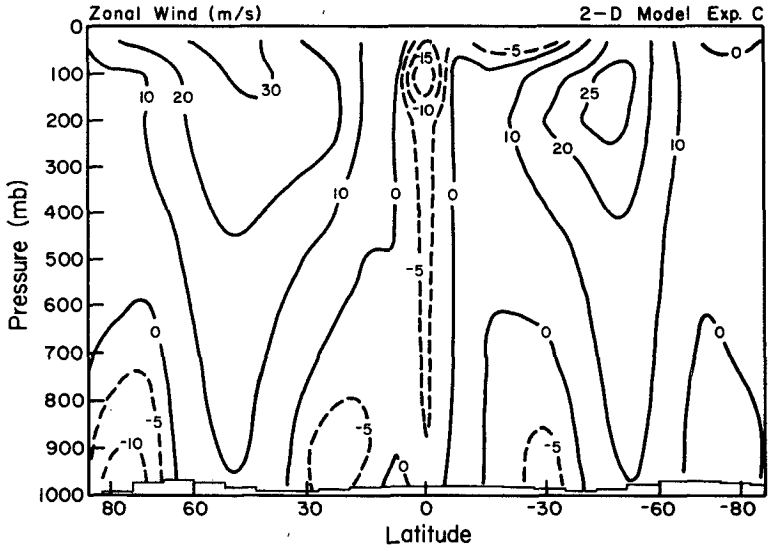

FIG. 7. As in Fig. 4, but with the meridional transport of angular momentum by eddies made independent of height (experiment C).

Finally, we mention one other experiment we carried out to evaluate the role of the eddy wind variances, $[u^{*2}]$ and $[v^{*2}]$, which appear in the meridional momentum equation. In this additional 2-D experiment, the wind variances were eliminated. (The total wind variance from the 3-D control run is illustrated in Part I.) The resulting changes in the general circulation were very small. Changes in the mean winds were only of order 0.1 to 0.2 m s^{-1}. Thus we do not bother to give any details of this experiment. It suffices to report that the eddy wind variances have a negligible influence on the general circulation.

4. Parameterization of the meridional eddy momentum flux

Our sensitivity experiments show that it is not necessary to parameterize the vertical eddy flux of momentum or the eddy wind variances. Thus we plan to leave these quantities out of the equations for our final model. In this section we turn our attention to the problem of developing an adequate parameterization of the meridional eddy flux of momentum. Throughout our development we will assume that the eddies responsible for this flux arise because of baroclinic instability, and that their dynamics is quasi-geostrophic.

The standard symbols used in the mathematical development are defined in the Appendix. In this section we define only symbols which are not standard. For convenience we use rectangular horizontal coordinates, but all the results can be generalized to spherical coordinates, and are used in that form in the 2-D model.

a. Parameterization in a dry atmosphere

The starting point for our development is Green's (1970) parameterization of the eddy momentum flux. This parameterization uses the quasi-geostrophic relation between the eddy fluxes of momentum, potential temperature, and quasi-geostrophic potential vorticity, ϕ, which in pressure coordinates takes the form

$$\frac{\partial}{\partial y}[u^*v^*] = f\frac{\partial}{\partial p}\frac{[v^*\theta^*]}{\sigma} - [v^*\phi^*]. \tag{1}$$

Green's parameterization assumes that θ and ϕ are conserved by the motions, so that the eddy transports of θ and ϕ can be parameterized by a mixing-length formulation,

$$[v^*\theta^*] = -K_{vy}\frac{\partial[\theta]}{\partial y} - K_{vp}\sigma \tag{2}$$

$$[v^*\phi^*] = -K_{vy}\frac{\partial[\phi]}{\partial y} - K_{vp}\frac{\partial[\phi]}{\partial p} \tag{3}$$

where K_{vy} and K_{vp} are components of the two-dimensional diffusion coefficient tensor. If these two mixing coefficients are known, then Eqs. (1) to (3) give an implicit parameterization of $[u^*v^*]$.

A problem arises whenever condensation effects are important, as they are in our model and in the real atmosphere. Under these conditions one can no longer expect θ and ϕ to be approximately conserved and the assumption behind Eqs. (2) and (3) breaks down. Nevertheless, it is useful to derive a parameterization for a dry atmosphere, and so in this subsection we will proceed as though Eqs. (2) and (3) are valid. We will take up the problem of how the parameterization has to be modified for a moist atmosphere in the next subsection.

In general one needs both K_{vy} and K_{vp} to calculate $[u^*v^*]$ from Eqs. (1) to (3). Green suggested parameterizations for these coefficients based on the assumption that the mixing was due to the most unstable baroclinic wave. However, his parameterizations left out some features of these waves of importance to us. They did not explicitly include the vertical structure of the mixing coefficients, and they left out the effect of β on this vertical structure. The latter effect is very important in cutting off the eddy transports due to baroclinic instability in low latitudes. Branscome (1983) has proposed a parameterization for the heat transports due to the most unstable baroclinic wave which does include these effects. Implicit in this parameterization is a parameterization of K_{vy} which we will therefore use as a starting point for our parameterization of K_{vy}.

Unfortunately, there is no equivalent parameterization of K_{vp} available. [Branscome's method leads to a trivial result for K_{vp}, i.e., $K_{vp} = 0$ (see Branscome, 1980).] However, as Green pointed out, one does not need K_{vp} in order to parameterize the *vertical integral* of $[u^*v^*]$. This is because the K_{vp} term in Eq. (3) is negligible—it is smaller than the K_{vy} term by a factor of order of the Rossby number—and because the boundary conditions on K_{vp},

$$K_{vp} \to 0 \quad \text{as} \quad p \to 0, p_s,$$

cause the K_{vp} term in Eq. (2) to drop out when Eq. (2) is integrated vertically. In particular, if we substitute into Eq. (2) the thermal wind relation,

$$R\frac{p^{\kappa-1}}{p_0{}^{\kappa}}\frac{\partial[\theta]}{\partial y} = f\frac{\partial[u]}{\partial p},$$

neglect the K_{vp} term in Eq. (3), substitute for the eddy fluxes from Eqs. (2) and (3) into Eq. (1), integrate Eq. (1) over all p and apply the boundary conditions on K_{vp}, we obtain

$$\frac{\partial}{\partial y}\int_0^{p_s}[u^*v^*]dp = -\left\{K_{vy}\frac{f^2p_0{}^{\kappa}}{\sigma R p^{\kappa-1}}\frac{\partial[u]}{\partial p}\right\}_{p=p_s} + \int_0^{p_s}K_{vy}\frac{\partial[\phi]}{\partial y}\,dp.$$

This can be simplified further, by substituting for the potential vorticity gradient,

$$\frac{\partial[\phi]}{\partial y} = \beta - \frac{\partial^2[u]}{\partial y^2} + \frac{f^2}{R}\frac{\partial}{\partial p}\frac{p_0^\kappa}{\sigma p^{\kappa-1}}\frac{\partial[u]}{\partial p}$$

and integrating by parts. The result is

$$\frac{\partial}{\partial y}\int_0^{p_s}[u^*v^*]dp = \int_0^{p_s}\left\{K_{vy}\left(\beta - \frac{\partial^2[u]}{\partial y^2}\right) - \frac{f^2 p_0^\kappa}{\sigma R p^{\kappa-1}}\frac{\partial[u]}{\partial p}\frac{\partial K_{vy}}{\partial p}\right\}dp. \quad (4)$$

Equation (4) shows that we only need an appropriate parameterization of K_{vy} in order to calculate the vertical mean of the eddy momentum flux. Since our experiment C showed that the vertical variations of $[u^*v^*]$ were not crucial to modeling the impact of $[u^*v^*]$ we will not attempt to parameterize K_{vp}. Rather, we will fix the vertical variations of $[u^*v^*]$ in our 2-D model, and parameterize only the vertical mean of the eddy momentum flux.

The vertical structure calculated in the 3-D control run has only weak latitudinal and seasonal variations (e.g., see Fig. 2). Therefore, for simplicity we decided to specify the same vertical structure to use in our 2-D model at all latitudes and seasons. For this structure we chose the global mean structure from the 3-D control run. This structure is shown in Table 2.

We now consider the parameterization of K_{vy}. Branscome's (1980) parameterization of K_{vy}, which we will denote by K_{BC}, is

$$K_{BC} = \frac{1}{\sqrt{2}}\left\langle\frac{\partial u}{\partial z}\right\rangle\frac{\langle N\rangle}{f}d^2 e^{-z/d}, \quad (5)$$

where the triangular brackets indicate a weighted vertical mean,

$$\langle x\rangle = \frac{\int_0^\infty xe^{-z/d}dz}{\int_0^\infty e^{-z/d}dz}, \quad (6)$$

d is the depth scale for the most unstable baroclinic wave,

TABLE 2. Mean vertical structure of the meridional eddy momentum flux from the 3-D control run.

Pressure (mb)	Normalized (u^*v^*)
27	.114
103	.393
201	1.000
321	.741
468	.440
634	.267
786	.175
894	.130
959	.134

$$d = \frac{\langle H\rangle}{[(1+\gamma)^2+1]^{1/2}-1}, \quad (7)$$

and γ is a nondimensional measure of β-effects,

$$\gamma = \frac{\beta\langle H\rangle\langle N^2\rangle}{f^2\langle\partial u/\partial z\rangle}. \quad (8)$$

In these formulas all the quantities retain their full latitudinal variation.

Branscome (1983) has shown that the corresponding parameterization of the eddy heat transport gives good results when compared with observations. However, this does not guarantee that K_{BC} will give good results for the eddy momentum transport. This is particularly true because the divergence of $[u^*v^*]$ is given by the difference of two terms which are comparable in size and involve K_{vy}. Therefore, even small errors in K_{vy} may lead to large errors in $[u^*v^*]$. It is instructive to substitute $K_{vy} = K_{BC}$ in Eq. (4) to see what Branscome's parameterization implies about the eddy momentum flux. For simplicity we neglect vertical variations in N, σ, $\partial[\theta]/\partial y$, and H, and neglect $\partial^2[u]/\partial y^2$ compared to β. The result is

$$\frac{\partial}{\partial y}\int_0^{p_s}[u^*v^*]dp = \int_0^{p_s}\beta K_{BC}\left\{1+\frac{1}{\gamma}-\left[\left(1+\frac{1}{\gamma}\right)^2+\frac{1}{\gamma^2}\right]^{1/2}\right\}dp. \quad (9)$$

The quantity in curly brackets in Eq. (9) is negative for all γ and is largest in magnitude for small γ. Thus, Eq. (9) implies that the most unstable wave always gives rise to a convergence of eddy momentum flux, with the convergence being a maximum where γ is a minimum. This result agrees qualitatively with numerical calculations of the eddy momentum flux produced by small amplitude baroclinic instabilities (e.g., Moura and Stone, 1976). Furthermore, it leads to estimates of the convergence in midlatitudes which are realistic. For example, if we use Oort and Rasmusson's (1971) analysis for the annual mean state at 50°N, we estimate from Eq. (9) that the vertical mean convergence is $\sim 10^{-5}$ sec^{-1}, comparable to the observed values. However, at the same time, Eq. (9) has the obvious defect that it predicts convergence at *all* latitudes; i.e., a parameterization based on $K_{vy} = K_{BC}$ would not conserve momentum globally.

Another potential problem with choosing $K_{vy} = K_{BC}$ is exposed by nonlinear calculations of the life cycles of baroclinic waves. Branscome's parameterization assumes that the vertical structure of the wave is given accurately by the linearized wave structure, whereas Simmons and Hoskins (1978) and Edmon et al. (1980) have shown that this structure changes markedly when nonlinear effects become important. In particular, the linear structure is only characteristic of the early stages

of the life cycle, while in the later, nonlinear stages the wave spreads into the upper troposphere and into lower latitudes. Since most of the heat transport does occur in the early stages, choosing $K_{vy} = K_{BC}$ is reasonable for parameterizing the eddy heat transport; but much of the eddy potential vorticity transport occurs in the later, nonlinear, stages of the life cycle, so choosing $K_{vy} = K_{BC}$ is not likely to work well for parameterizing either the eddy potential vorticity transport, or the eddy momentum transport.

The foregoing picture of the life cycle of a baroclinic instability does suggest one way of improving the parameterization of K_{vy}. We let

$$K_{vy} = K_{BC} + K_{NL}, \tag{10}$$

where K_{NL} is a correction to the coefficient meant to allow for modifications of the wave structure associated with the mature stage of the instability's life cycle. To reflect the deeper structure in the later stages of the life cycle, we choose K_{NL} to be independent of height. Referring to Eq. (4), we see that K_{NL} will then give rise solely to a divergence of the eddy momentum flux, and tend to balance the convergence associated with K_{BC}. Thus, a judicious construction of K_{NL} will enable us to guarantee global conservation of momentum, as well as to include nonlinear effects.

To parameterize the meridional variations of K_{NL}, we invoke wave propagation theory. In uniform flow, eastward-traveling waves can propagate meridionally as long as the flow is westerly, but not when the flow is easterly (Charney, 1973). Therefore, we model the spreading out of the initial wave structure by assuming that the wave propagates meridionally through the regions of westerly winds, but does not extend very far into regions of easterly winds. In particular, we approximate

$$K_{NL} = \begin{cases} K_0, & [\bar{u}] > 0 \\ K_0 e^{-y_0/L}, & [\bar{u}] < 0 \end{cases}, \tag{11}$$

where K_0 is a constant, the bar indicates a vertical mean,

$$[\bar{u}] = \frac{1}{p_s}\int_0^{p_s} [u]dp,$$

y_0 is the distance into the region of easterlies from the latitude where $[\bar{u}] = 0$, and L is a characteristic decay scale in the evanescent region. This decay scale depends on the phase speed of the waves, but it is typically somewhat less than the radius of deformation. As a reasonable initial estimate for this scale, we choose

$$e^{-\Delta/L} = \frac{1}{4}, \tag{12}$$

where Δ is the meridional resolution of our model (870 km). This choice corresponds to a value for L of 626 km. We will examine the sensitivity of our results to this choice in the next subsection.

Finally K_0 is chosen so that momentum is conserved globally. In practice the eddy flux of momentum across the equator is always negligible (e.g., see Fig. 2); i.e., momentum is conserved separately in each hemisphere, and there is no reason why K_0 should have the same value in both the winter and summer hemispheres. Thus we allow K_0 to have different values in each hemisphere, and determine these values by requiring that the integral of Eq. (4) over each hemisphere be zero.

Equations (4), (10), (11) and (12), along with the appropriate definitions, the requirement of hemispheric momentum conservation, and the vertical structure given in Table 2, now completely specify the parameterization of $[u^*v^*]$ for a dry atmosphere. In Experiment D we tested this parameterization in our (moist) 2-D model. The results for the vertically integrated eddy meridional momentum transport are shown in Fig. 8, where they are compared with the results from the 3-D control. Although the parameterization simulates the latitudinal variations of the eddy momentum flux quite well, the simulated magnitude of the eddy flux is too small. The peak value of the parameterized eddy flux in the Northern Hemisphere is only 34% of that in the control run, and in the Southern Hemisphere only 16% of that in the control run. Errors in the 2-D simulation of other fields, such as σ, can only account for a small portion of this discrepancy. We conclude that the parameterization itself must be at fault. The fact that the parameterization is poorest in the summer hemisphere where the moisture effects are greatest does suggest that the neglect of condensation effects in the derivation of the parameterization is one source of the error.

b. Parameterization in a moist atmosphere

Here we generalize the parameterization to include the effects of condensation associated with the large-scale eddies. When condensation is important, we can no longer assume that θ and ϕ are conserved quantities, and the parameterizations for the corresponding eddy fluxes, Eqs. (2) and (3), are no longer appropriate. However, if we can define alternate variables which are conserved by the eddies even when condensation occurs, then mixing-length parameterizations can still be used.

An obvious alternate variable that can replace the potential temperature is the equivalent potential temperature, θ_e. We approximate the moisture conservation equation with the aid of the quasi-geostrophic approximation,

$$\frac{\partial q}{\partial t} + u\frac{\partial q}{\partial x} + v\frac{\partial q}{\partial y} + \omega\frac{\partial q_s}{\partial p} = -\frac{Q}{L_v}, \tag{13}$$

where Q represents the diabatic heating due to the large-scale condensation associated with the eddies. Using this equation to eliminate the diabatic heating from the heat conservation equation, we obtain

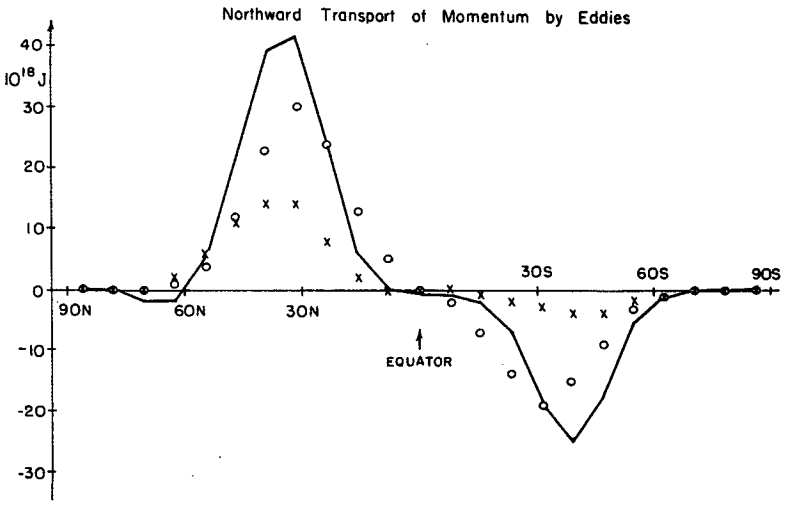

FIG. 8. Northward transport of momentum by eddies vs latitude from the 3-D control run (solid line) and from the 2-D experiments with parameterized meridional eddy transports of angular momentum: experiments D (×'s) and E (O's).

$$\frac{\partial \theta_e}{\partial t} + u\frac{\partial \theta_e}{\partial x} + v\frac{\partial \theta_e}{\partial y} + \sigma_e \omega = 0 \tag{14}$$

where

$$\sigma_e = \sigma + \frac{L_v}{c_p}\left(\frac{p_0}{p}\right)^{\kappa}\frac{\partial q_s}{\partial p}.$$

Equation (14) is, of course, just the conservation form of the quasi-geostrophic thermodynamic equation. Thus, we can assume a mixing length parameterization for the eddy flux of θ_e,

$$[v^*\theta_e^*] = -K_{vy}\frac{\partial [\theta_e]}{\partial y} - K_{vp}\sigma_e. \tag{15}$$

For the second alternate variable we need a variable analogous to the quasi-geostrophic potential vorticity. If we use Eq. (14) to substitute for ω in the quasi-geostrophic vorticity equation, we obtain

$$\left(\frac{\partial}{\partial t} + u\frac{\partial}{\partial x} + v\frac{\partial}{\partial y}\right)\left\{f + \frac{\partial v}{\partial x} - \frac{\partial u}{\partial y} + f\frac{\partial}{\partial p}\frac{\theta_e}{\sigma_e}\right\} = \frac{L_v}{c_p}\frac{1}{\sigma_e}\left(\frac{p_0}{p}\right)^{\kappa}\left(\frac{\partial u}{\partial p}\frac{\partial q}{\partial x} + \frac{\partial v}{\partial p}\frac{\partial q}{\partial y}\right). \tag{16}$$

Thus the equivalent potential vorticity, defined by replacing θ and σ by θ_e and σ_e in the definition of potential vorticity (Saltzman, 1962), is not, in general, a conserved quantity. However, there is an approximation for q suggested by Leovy (1973) for parameterizing eddy moisture effects that achieves the desired simplification. Following Leovy, we assume that the eddy fluctuations in relative humidity are small compared to the eddy fluctuations in specific humidity, and that the eddy temperature fluctuations are small compared to the absolute temperatures, so that we can linearize the Clausius–Clapeyron equation. As a result we can approximate

$$q \approx r\frac{\partial S(T_s)}{\partial T}T, \tag{17}$$

where r is the basic state relative humidity and S is the saturated specific humidity of the basic state. In this approximation the horizontal variations in q are just proportional to those in T, and, therefore, because of the thermal wind relations, the two terms on the right-hand side of Eq. (16) cancel. Consequently, the equivalent potential vorticity

$$\Pi = f + \frac{\partial v}{\partial x} - \frac{\partial u}{\partial y} + f\frac{\partial}{\partial p}\frac{\theta_e}{\sigma_e}, \tag{18}$$

is (approximately) conserved by geostrophic motions. Thus, we can again use a mixing length parameterization. As in the dry case, the K_{vp} term is smaller than the K_{vy} term in the parameterization of the eddy flux of Π by a factor of the order of the Rossby number, so we may write

$$[v^*\Pi^*] \approx -K_{vy}\frac{\partial [\bar{\Pi}]}{\partial y}. \tag{19}$$

To complete the parameterization with condensation effects included, we need to generalize the form of the quasi-geostrophic relation between the eddy fluxes. This is straightforward because Eq. (17) allows us to write

$$\theta_e = \theta(1 + M) \tag{20}$$

where

$$M = \frac{L_v}{c_p} r\frac{\partial S}{\partial T}. \tag{21}$$

Since M is just a function of pressure, the generalized form can be derived in the same way as the original form, Eq. (1). We simply evaluate Π^* from Eq. (18), multiply Π^* by v^*, apply the zonal averaging operator, integrate by parts, and substitute from the continuity and thermal wind relations. The result is

$$\frac{\partial}{\partial y}[u^*v^*] = f\frac{\partial}{\partial p}\frac{[v^*\theta_e^*]}{\sigma_e} - [v^*\Pi^*]. \tag{22}$$

As in the dry atmosphere case, we will specify the vertical structure of $[u^*v^*]$ from Table 2 and only attempt to parameterize the vertical integral of $[u^*v^*]$. The equation for the vertical integral is derived in a way exactly analogous to the derivation of Eq. (4) for the dry case. In the derivation, Eqs. (1), (2), and (3) are replaced by Eqs. (22), (15), (19) along with the appropriate definitions. The result is

$$\frac{\partial}{\partial y}\int_0^{p_s}[u^*v^*]dp = \int_0^{p_s}\left\{K_{vy}\left(\beta - \frac{\partial^2[u]}{\partial y^2}\right) - \frac{(1+M)f^2p_0^{\kappa}}{R\sigma_e p^{\kappa-1}}\frac{\partial[u]}{\partial p}\frac{\partial K_{vy}}{\partial p}\right\}dp. \tag{23}$$

If we replace σ_e by σ and set $M = 0$, we retrieve the result for the dry atmosphere.

Since it is the last term in the integrand of Eq. (23) which leads to a convergence of the eddy momentum flux, and since $M > 0$ and $\sigma_e < \sigma$, we see that, *all else being equal,* including the large-scale condensation effects increases the eddy momentum flux convergence. This result is related to the result found by Salustri and Stone (1984), that, all else being equal, these effects increase the total eddy forcing of the zonal wind and temperature fields. In fact, Eq. (22) can be rewritten as

$$[v^*\Pi^*] = \nabla\cdot\mathbf{F}_M, \tag{24}$$

where $\mathbf{F}_M$ is the "moist" Eliassen–Palm flux defined by Stone and Salustri. This generalization of the relation between the quasi-geostrophic eddy potential vorticity flux and the Eliassen–Palm flux is only made possible by Leovy's approximation for the moisture fluctuations, Eq. (17).

The whole formalism as presented for generalizing Green's (1970) approach to parameterizing the eddy momentum flux is crucially dependent on the validity of Leovy's approximation. The two necessary assumptions are, a priori, at least plausible. Typical values of the temporal standard deviation of temperature in the atmosphere are 3° to 5°K (Oort and Peixoto, 1983), so linearizing the Clausius–Clapeyron equation is a reasonable first approximation. Also, the presence of an essentially infinite source of water at the surface does tend to limit fluctuations in relative humidity. One quantitative test of the approximation can be made by using it to calculate the eddy moisture flux. From Eq. (17) we derive

$$[v^*q^*] = r\frac{\partial S(T_S)}{\partial T}[v^*T^*]. \tag{25}$$

Thus, by comparing the eddy moisture flux calculated from this equation with the same flux calculated from observations, or from an explicit 3-D simulation of the eddies, we can get a direct test of Eq. (17).

Mullan (1979; also see Stone, 1984) showed that Eq. (25) did give reasonable results when compared to observations in mid- and high latitudes, but not in the subtropics; the breakdown in the subtropics is apparently caused by the zonal variations of relative humidity associated with ocean-land contrasts. Since our 2-D model a priori excludes such effects, our parameterization is meant only to simulate the effects of transient large-scale eddies. Leovy's approximation should work better for simulating just these effects.

Figure 9 shows the eddy latent heat flux, $L_v[v^*q^*]$, calculated directly from the 3-D control run, while Fig. 10 shows $L_v[v^*q^*]$, calculated from Eq. (25) using the $[v^*T^*]$ calculated from the 3-D control run. In the latter calculation, we allowed r and T_s to retain their latitudinal variations, i.e., we assumed that Leovy's approximation can be applied *locally.* On the whole, the two fields agree fairly well. The most notable discrepancy is that the parameterized flux does not have the double maximum in the vertical structure that appears in the explicitly calculated flux. On the other hand, the parameterization does reproduce the latitudinal variations and the magnitude of the flux quite well. Because of the lack of a double maximum, the vertically integrated transport is less than that calculated explicitly, but only by 20%. [We note that the double maximum also appeared in the January simulation with the semispectral model using realistic lower boundary conditions, but does not appear in observations (Oort and Peixoto, 1983). Thus, the double maximum in the 3-D model does not appear to be realistic. Also the semispectral model with realistic lower boundary conditions calculated a total eddy flux about 10% larger than the observed January flux.] We conclude that Leovy's approximation is a reasonable one to use for parameterizing moisture fluctuations in large-scale transient eddies.

To complete the parameterization of $[u^*v^*]$ when eddy condensation is important we still must specify K_{vy}. We expect the main features of the parameterization of K_{vy}, developed here for a dry atmosphere, to be unchanged. First, Branscome's K_{BC} primarily reflects mixing in the earlier, quasi-linear stages of the baroclinic waves, when condensation effects are relatively unimportant. Second, the decay of the correction coefficient K_{NL} in regions of easterlies occurs outside the regions where eddy condensation is important. And third, the magnitude of K_{NL} is determined by the requirement of momentum conservation, which is not affected by whether or not condensation occurs. Thus, we adopt the same parameterization of K_{vy} for a moist

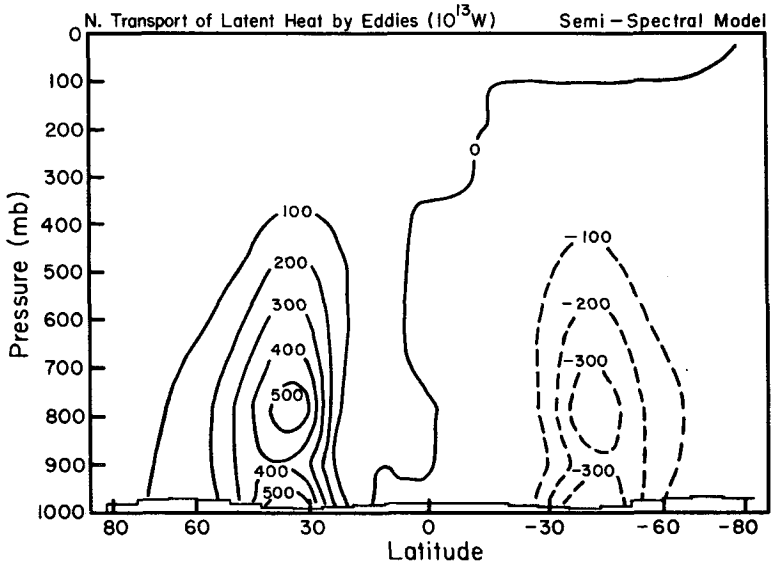

FIG. 9. Pressure–latitude cross section of the meridional transport of latent heat by eddies calculated from the 3-D control run. Units = 10^{13} w per unit σ.

atmosphere as for a dry atmosphere: it is calculated from Eqs. (10), (11), and (5), and then substituted in Eq. (23) to obtain the vertical integral of $[u^*v^*]$. Again, we allow M and σ_e to retain their latitudinal variations.

In experiment E with the 2-D model, we tested this parameterization of $[u^*v^*]$. The results for the total eddy momentum transport are shown in Fig. 8, where they are compared with the results from the 3-D control run and from experiment D (which used the parameterization for a dry atmosphere). We see that the moist parameterization gives magnitudes closer to those in the 3-D control run than the dry parameterization, as expected. Both the M and σ_e factors in Eq. (23) are important in causing the increase in magnitude. The peak values in the moist parameterization are about 75% of the peak values in the 3-D control run in both hemispheres. (We note that this does not mean that the eddy momentum fluxes are much stronger than they would be if the atmosphere were dry, because the calculations with the dry parameterizations used data from a moist model. In a truly dry atmosphere the static stability would be smaller and the meridional

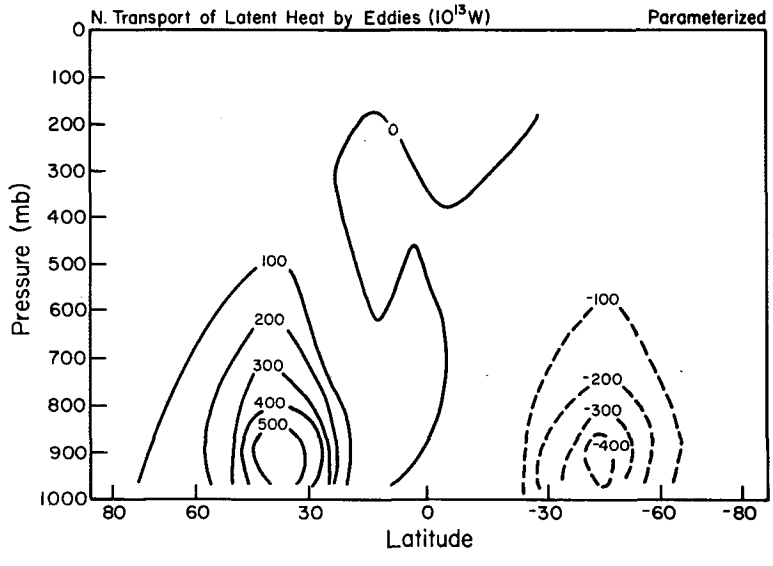

FIG. 10. As in Fig. 9, but calculated from Eq. (25).

temperature gradient would be larger, and both of these effects would increase the eddy momentum flux calculated from the dry parameterization.) The parameterization simulates the latitudinal and seasonal variation fairly well. In experiment E the values of K_0 calculated by the parameterization were 1.3×10^6 m^2 s^{-1} in the Northern Hemisphere and 1.2×10^6 m^2 s^{-1} in the Southern Hemisphere. Typical values of K_{BC} at $z = 0$ were four times larger.

Another important test of our parameterization of the eddy momentum flux is how well it simulates the impact of the correct eddy momentum flux on the general circulation. Figure 11 illustrates the zonal wind field produced by the parameterization in experiment E. This may be compared with the zonal wind field produced by the "correct" eddy momentum flux (Fig. 4) and that produced when the eddy flux is omitted (Fig. 6). We see that the parameterization does simulate most of the desired impact. 1) The secondary westerly jets near the poles and at the equator have been eliminated; 2) the strength of the easterly jet in the equatorial stratosphere has been reduced; 3) the strengths of the two midlatitude jets now agree with those in the control run within the natural monthly variability (a few percent); and 4) the jet streams have been displaced poleward. There are still some notable discrepancies. The Southern Hemisphere jet is about one grid point north of where it should be. (However, it is worth noting that when the 3-D semispectral model is run for January conditions with realistic lower boundary conditions, its Southern Hemisphere jet is about one grid point *south* of where it should be according to observations—see Part I. Thus the discrepancy may be the fault of the 3-D model rather than the parameterization.) Also, the zonal winds in high northern latitudes are still stronger than they should be. Associated with this latter discrepancy are temperatures in high northern latitudes which are still colder than in the control run. However, this discrepancy has been greatly reduced compared to the experiment with no eddy momentum flux. For example, the mean temperature error at 82°N was reduced from 10° to 3°C by the parameterized eddy momentum flux.

Next we compare the meridional circulations produced by the moist parameterization in experiment E with those calculated in the 2-D control run. Figures 12 and 13 show the streamfunction for the zonal mean meridional and vertical winds from these two experiments, respectively. The experiment with the parameterized transport simulates the double intertropical convergence zone (ITCZ) and the Hadley cells with about the right strengths. The Northern Hemisphere Hadley cell and ITCZ have approximately the right locations, but the Southern Hemisphere ITCZ and Hadley cell, like the Southern Hemisphere jet stream, are about one grid point too far north. Perhaps the most notable discrepancy in experiment E is the appearance of a relatively weak reversed cellular circulation near the equator within the Northern Hemisphere Hadley cell. As a result of this cell the sinking motion between the two ITCZ's, which is rather weak in the control run, is greatly enhanced in experiment E. Also, the Ferrel cells in experiment E have only about one-half the strength of those in the control run. (The Ferrel cells are very sensitive to errors in the magnitude of $[u^*v^*]$ because they represent the net effect of forcings by diabatic heating and eddies, which have opposite signs.)

We also performed some experiments to determine the sensitivity of the parameterization of the eddy mo-

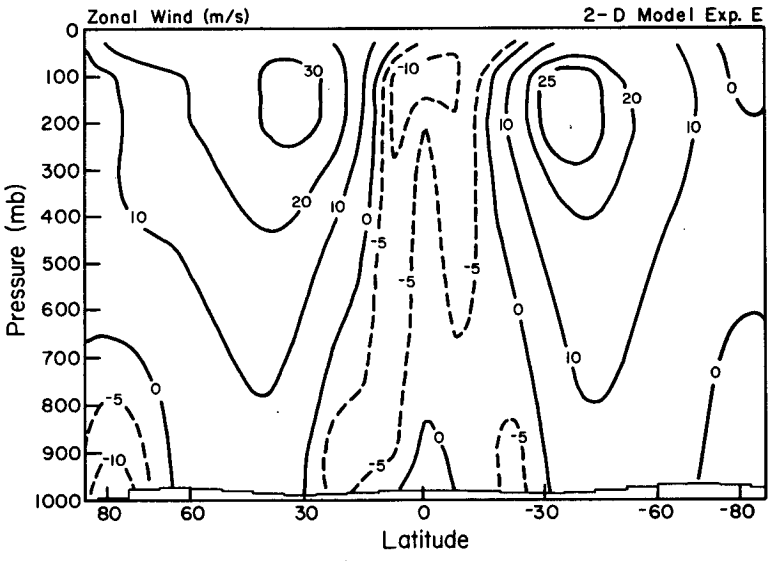

FIG. 11. As in Fig. 4, but from experiment E.

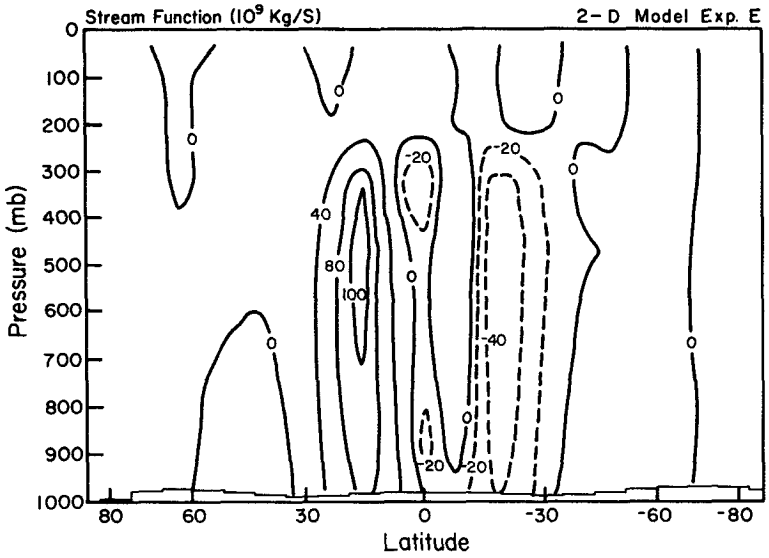

FIG. 12. Pressure–latitude cross section of the zonal mean streamfunction from experiment E. Units = 10^9 kg s^{-1}.

mentum transport in a moist atmosphere to some of the uncertainties in its formulation. The whole formulation is based on the quasi-geostrophic approximation, which we expect to break down in the planetary boundary layer, both because of dissipation and because σ_e becomes relatively small in the boundary layer. We therefore repeated experiment E but with the model's two lowest layers ($p > 840$ mb) omitted from the calculation of the vertical integrals in Eq. (23). The results for the eddy momentum transport are shown in Fig. 14. We see that including the boundary layer has very little effect on the parameterized eddy momentum transport.

We also repeated experiment E with different choices for L, the decay scale for the correction coefficient in regions of easterlies. We recall that in the original experiment E, we chose $L = 626$ km. Figure 14 shows how the eddy momentum transport changes when L is decreased to 417 km ($\frac{2}{3}$ of 626) or increased to 939 km ($\frac{3}{2}$ of 626). The transport in the winter hemisphere is not sensitive to the different choices of L, with the changes in the transport being 10% or less. There is

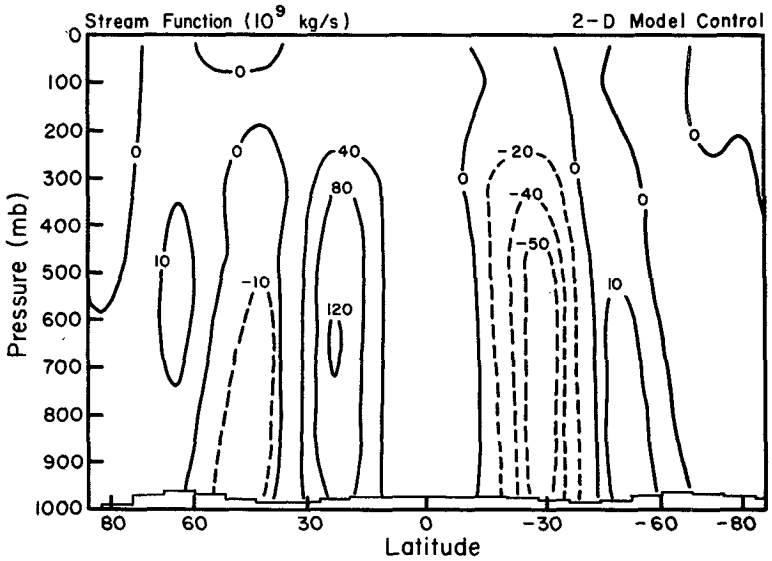

FIG. 13. As in Fig. 12, but from the 2-D control run.

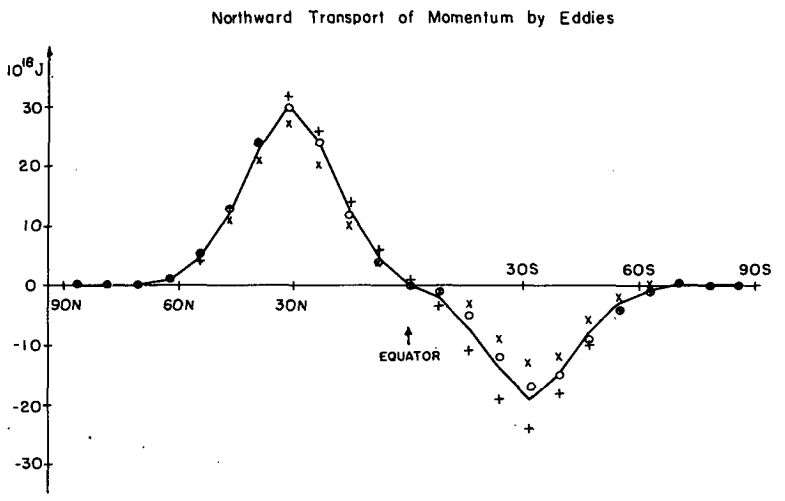

FIG. 14. Northward transport of momentum by eddies vs latitude from experiment E (solid line) and from experiments in which experiment E was repeated with 1) the boundary layer omitted from the calculation of the transport (circles); 2) L decreased to 417 km (×'s); and 3) L increased to 939 km (pluses).

more sensitivity in the summer hemisphere where changes as large as 30% occur. Clearly, it would be desirable to have a parameterization for L, itself, in the summer hemisphere. However, this lack is mitigated by the fact that the general circulation in the summer hemisphere is relatively insensitive to the eddy momentum transport. For example, the changes in L only led to changes in the strength of the Southern Hemisphere jet stream and Hadley cell circulation of 2 and 10%, respectively. Thus, we consider our original choice of L to be satisfactory.

5. Summary and conclusions

We have used perpetual January simulations with a 2-D model to study the sensitivity of the general circulation to the various eddy forcing terms which enter the zonally averaged momentum conservation equations. We found that the vertical eddy flux of angular momentum and the meridional and zonal wind variances have negligible effects on the general circulation. Thus, we plan to leave these forcing terms out of the final form of our 2-D model. By contrast, the meridional eddy flux of angular momentum has a major effect. Our sensitivity experiments essentially confirm Schneider's (1984) results on the impact of this flux on the annual mean general circulation.

In addition, our sensitivity experiments showed that the vertical structure of the meridional eddy flux has relatively little impact on the general circulation, presumably because the vertical structure is strongly constrained by the thermal wind relation and surface friction. Because of this result we do not plan to parameterize the vertical structure of the eddy momentum flux in the final form of our model. Rather, this structure will be specified from our 3-D model calculations; i.e., we will use the structure given in Table 2.

On the other hand, a parameterization of the vertically integrated meridional eddy flux of angular momentum is clearly necessary in order to simulate accurately the general circulation and its response to climate changes. We have presented a new parameterization of this eddy momentum transport, one which is intended to represent the transport due to large-scale transient eddies arising from baroclinic instability. We took Green's (1970) method of calculating this transport as our starting point, and generalized it to include the effect of condensation associated with the large-scale eddies. We approximated this effect by using Leovy's (1973) approximation for the eddy fluctuations in specific humidity. With this approximation the equivalent potential vorticity (Saltzman, 1962) is conserved by geostrophic motions even when large-scale condensation is present. The definition of equivalent potential vorticity is analogous to the definition of the usual quasi-geostrophic potential vorticity, but the potential temperature is replaced by the equivalent potential temperature. We tested Leovy's approximation by using it to calculate the eddy latent heat flux and comparing the result to an explicit 3-D simulation of the flux. The comparison indicates that the approximation works well.

Leovy's approximation also allows us to generalize the relationship between quasi-geostrophic potential vorticity and the Eliassen–Palm flux to include condensation effects. One simply replaces the potential temperature and potential vorticity by the corresponding "equivalent" quantities. Thus, when large-scale

condensation is present, one can still calculate the eddy momentum flux from the eddy fluxes of two conserved quantities, equivalent potential temperature and equivalent potential vorticity. We parameterized the eddy transports of the two conserved quantities by mixing length expressions. The eddy mixing coefficient was taken to be equal to Branscome's parameterization plus a correction. The correction is chosen so as to modify the structure of the coefficient in a way which allows for nonlinear effects on the eddy structure, to a first approximation, and which also allows global momentum to be conserved.

Finally, we tested the whole parameterization for the meridional eddy momentum transport by using it in a perpetual January simulation with our 2-D model and comparing the results with a parallel 3-D simulation which calculated the eddy momentum transport explicitly. The parameterization simulated the latitudinal and seasonal variations and the magnitude of the eddy momentum flux reasonably well, once the condensation effects were included. The main discrepancy was that the parameterization underestimated the eddy momentum transport by about 25%, which led to corresponding discrepancies in the 2-D simulation of the general circulation. We note that GCM simulations of the real atmosphere frequently have comparable errors in the eddy momentum transport, even with resolutions as high as 250 km (e.g., Kasahara and Washington, 1971; Somerville et al., 1974; Manabe and Terpstra, 1974; and Stone et al., 1977). In addition, our 2-D simulation was carried out in a way which probably overestimates the error in the parameterization. In particular, the 2-D simulation omitted the feedback between the eddy heat fluxes and the general circulation, and these feedbacks are generally strongly negative (Stone, 1984). Thus, we consider the parameterization to be an adequate one to use in the final form of our 2-D model.

Acknowledgments. We are indebted to Lee Branscome for many useful discussions. This work was supported principally by the NASA Climate Program managed by Robert Schiffer.

APPENDIX

List of Symbols

c_p	specific heat at constant pressure
f	Coriolis parameter
H	density scale height
L_v	latent heat of vaporization
N	Brunt–Väisälä frequency
p	pressure
p_0	reference pressure
p_s	surface pressure
q	deviation of the specific humidity from q_s
q_s	specific humidity of the basic state; a function of p only
r	relative humidity
R	perfect gas constant
T	deviation of the temperature from T_s
T_s	temperature of the basic state; a function of p only
u	zonal wind
v	meridional wind
y	meridional coordinate
z	vertical coordinate
β	df/dy
κ	R/C_p
ϕ	quasi-geostrophic potential vorticity
σ	$d\theta_s/dp$
σ_e	$\sigma + \frac{L_v}{c_p}\left(\frac{p_0}{p}\right)^\kappa \frac{dq_s}{dp}$
θ	potential temperature deviation, $\left(\frac{p_0}{p}\right)^\kappa T$
θ_e	equivalent potential temperature deviation, $\theta + \frac{L_v}{C_p}\left(\frac{p_0}{p}\right)^\kappa q$
ω	vertical velocity in pressure coordinates
$[\ ]$	zonal mean
$(\ )^*$	deviation from the zonal mean

REFERENCES

Branscome, L. E., 1980: Scales and structures of baroclinic waves and their influence on climatic states. Ph.D. dissertation, MIT, Cambridge, MA, 201 pp.

——, 1983: A parameterization of transient eddy heat flux on a beta-plane. *J. Atmos. Sci.*, **40,** 2508–2521.

Charney, J. G., 1973: Planetary Fluid Dynamics. *Dynamic Meteorology,* P. Morel, Ed., D. Reidel, 97–351.

Edmon, Jr., H. J., B. J. Hoskins and M. E. McIntyre, 1980: Eliassen-Palm cross sections for the troposphere. *J. Atmos. Sci.*, **37,** 2600–2616.

Green, J. S. A., 1970: Transfer properties of the large-scale eddies and the general circulations of the atmosphere. *Quart. J. Roy. Meteor. Soc.*, **96,** 157–185.

Hansen, J., G. Russell, D. Rind, P. Stone, A. Lacis, S. Lebedeff, R. Ruedy and L. Travis, 1983: Efficient three dimensional global models for climate studies: Models I and II. *Mon. Wea. Rev.*, **111,** 609–662.

Kasahara, A., and W. M. Washington, 1971: General circulation experiments with a six-layer NCAR model, including orography, cloudiness and surface temperature calculations. *J. Atmos. Sci.*, **28,** 657–701.

Leovy, C. B., 1973: Exchange of water vapor between the atmosphere and surface of Mars. *Icarus,* **18,** 120–125.

Manabe, S., and Terpstra, T. B., 1974: The effects of mountains on the general circulation of the atmosphere as identified by numerical experiments. *J. Atmos. Sci.*, **31,** 3–42.

Moura, A. D., and P. H. Stone, 1976: The effects of spherical geometry on baroclinic instability. *J. Atmos. Sci.*, **33,** 602–616.

Mullan, A. B., 1979: A mechanistic model for mid-latitude mean temperature structure. Ph.D. dissertation, MIT, Cambridge, MA, 248 pp.

Oort, A. H., and E. M. Rasmusson, 1971: Atmospheric circulation statistics. NOAA Prof. Pap. No. 5, U.S. Dept. of Commerce, Washington, DC, 323 pp.

——, and J. P. Peixoto, 1983: Global angular momentum and energy balance requirements from observations. *Adv. Geophys.*, **25**, 355–490.

Saltzman, B., 1962: Empirical forcing functions for the large-scale mean disturbances in the atmosphere. *Geofis. Pura Appl.*, **52**, 173–188.

——, 1978: A survey of statistical-dynamical models of the terrestrial climate. *Adv. Geophys.*, **20**, 183–304.

Salustri, G., and P. H. Stone, 1983: A diagnostic study of the forcing of the Ferrel Cell by eddies with latent heat effects included. *J. Atmos. Sci.*, **40**, 1101–1109.

Schneider, E. K., 1984: Response of the annual and zonal mean winds and temperatures to variations in the heat and momentum sources. *J. Atmos. Sci.*, **41**, 1093–1115.

Simmons, A. J., and B. J. Hoskins, 1978: The life cycles of some nonlinear baroclinic waves. *J. Atmos. Sci.*, **35**, 414–432.

Somerville, R. C. J., P. H. Stone, M. Halem, J. E. Hansen, J. S. Hogan, L. M. Druyan, G. Russell, A. A. Lacis, W. J. Quirk and J. Tenenbaum, 1974: The GISS model of the global atmosphere. *J. Atmos. Sci.*, **31**, 84–117.

Starr, V. P., J. P. Peixoto and J. E. Sims, 1970: A method for the study of the zonal kinetic energy balance in the atmosphere. *Pure Appl. Geophys.*, **80**, 346–358.

Stone, P. H., 1984: Feedbacks between dynamical heat fluxes and temperature structure in the atmosphere. *Climate Processes and Climate Sensitivity Geophys. Monogr.* 29, Amer. Geophys. Union, 6–17.

——, and G. Salustri, 1984: Generalization of the quasi-geostrophic Eliassen-Palm flux to include eddy forcing of condensation heating. *J. Atmos. Sci.*, **41**, 3527–3536.

——, S. Chow and W. J. Quirk, 1977: The July climate and a comparison of the January and July climates simulated by the GISS general circulation model. *Mon. Wea. Rev.*, **105**, 170–194.

Yao, M.-S., and P. H. Stone, 1987: Development of a two-dimensional zonally averaged statistical-dynamical model. Part I: The parameterization of moist convection and its role in the general circulation. *J. Atmos. Sci.*, **44**, 65–82.